

Summary of HST Proper Motion Measurements

May 24, 2018

Canes Venatici I: This galaxy is at moderately high galactic latitude $(l,b) = (74.3^\circ, +79.8^\circ)$ and has a distance from the Sun of 218 ± 10 kpc (McConnachie 2012). It has a heliocentric radial velocity of 30.9 ± 0.6 km/s (Simon & Geha 2007). With an M_V of -8.6 , it is among the most luminous of the satellite galaxies found in the SDSS.

We have an exceptional four fields in this galaxy, which are shown in the figure below. The fields are numbered from 1 to 4 starting from the westernmost and proceeding to the easternmost field.

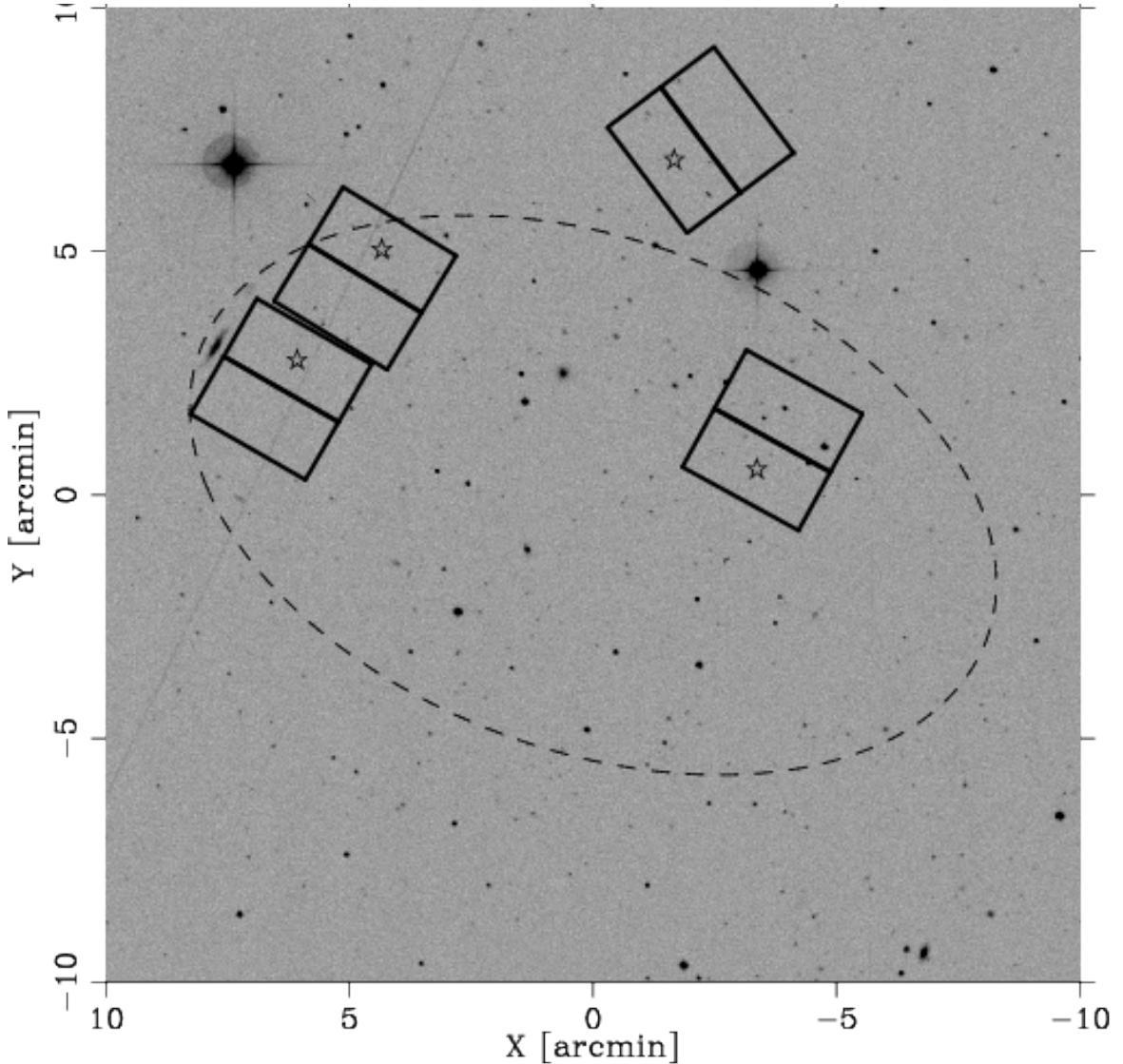


Figure 1: Fields in CVn I. The star indicates the QSO and is in the s chip. We call the other chip t. North is up and east is to the left. The dashed ellipse shows the half-light radius of the galaxy.

TABLE 1. Information about CVn I Pointings and Images

Pointing	R.A. (J2000.0)	Decl. (J2000.0)	Date yyyy – mm – dd	(X_Q, Y_Q) (pix, pix)	PA (deg.)	T_{exp} (s)
(1)	(2)	(3)	(4)	(5)	(6)	(7)
CVn I-1	13:27:44.9	+33:33:39.3	2009 – 12 – 28	(2035.66, 1021.70)	151	$3 \times 895,9 \times 932$
			2013 – 01 – 06	(2039.13, 1016.81)	151	$3 \times 887,9 \times 924$
CVn I-2	13:27:53.0	+33:40:10.0	2010 – 02 – 12	(2039.34, 1029.20)	127	$4 \times 639,8 \times 667$
			2013 – 02 – 14	(2038.51, 1028.14)	127	$3 \times 632,1 \times 605,$ 8×660
CVn I-3	13:28:21.9	+33:38:9.6	2010 – 07 – 20	(2036.82, 1013.46)	-31	$6 \times 383,12 \times 402$
			2012 – 06 – 22	(2038.92, 1012.66)	-31	$6 \times 377,12 \times 660$
CVn I-4	13:28:30.2	+33:35:53.6	2010 – 07 – 17	(2037.92, 1015.34)	-30	$5 \times 486,10 \times 508$
			2012 – 06 – 11	(2040.33, 1013.94)	-30	$5 \times 479,10 \times 501$

The QSO in Field 1 is a clearly extended galaxy and was treated as a galaxy (meaning it has its own individual psf). It was the faintest and reddest of the QSO's in our sample, which allowed the long exposure times in this field. The QSO's in Fields 2 and 3 were treated as stars (fit with the stellar psf). The QSO in field 4 appears stellar, but increased in brightness between the first and 2nd epoch by so much that it is close to saturating. It actually is saturated in two of the 2nd-epoch images (so not measured in those images). I first reduced that field treating the QSO as a star, but then re-reduced the field treating it as a galaxy to see if it had affected the stellar psf. The proper motion based on galaxies did not change at all and the proper motion based on the QSO changed by about 1 sigma (coming into better agreement with the other measurements).

We take the average positions determined at the second epoch and transform these into the coordinate system of the first epoch using the most general second-order transformation (i.e., including all quadratic terms). If the sample of stars is large and the residuals of the transformation suggest that it is necessary, a term cubic in x is also included in the transformation of the x positions. We have already corrected the positions using known distortions in the camera and filter (which are not that well known for the F350LP filter that we are using), but still find that a transformation with terms of higher order than first is necessary to remove trends in the residuals (when we have enough stars to see them). The higher-order terms could come from our use of a constant PSF to fit positions despite clear variations of the shape of the PSF with position in the frame (and between individual images). I have done some experimentation with reducing the number of terms in the transformation when the number of members stars is small and have not found a significant change in the measured proper motion.

When doing the transformation between epochs we iteratively reject stars with large deviations, assuming that these are non-members. Our program actually accepts a list of stars with large proper motions that are excluded from the beginning. This is useful, particularly with a small sample of stars, in preventing the initial transformation from being distorted by very large deviations. We include an additional uncertainty in the position of objects that is added in quadrature to the coordinate position uncertainties with the goal of making the chi-square of the fitted transformation one per degree of freedom. For reasons that I do not understand, the size of this additional uncertainty varies from field to field. It could have to do with how the positions of bright stars interact with the correction for camera/filter distortion or with the errors induced by the spatially variable PSF. In some fields even an additional uncertainty of 0.0 leaves the chi-square smaller than the number of degrees of freedom. Since our proper motions measured in different fields for the same galaxy tend not to agree within their uncertainties, I have adopted a minimum additional uncertainty of 0.0025 pixel on the grounds that it is likely a bad idea to put too much weight on a few high-S/N stars that may be affected by systematic errors, particularly when the sample of stars is not that large. There were also cases where a small additional uncertainty excluded what looked to be likely member stars and in those cases I increased the uncertainty until the stars were members.

The table below gives the number of stars, N_s , the number of member stars, N_m , the adopted additional uncertainty, the number of terms in the fitted transformation, N_f , the total χ^2 and number of degrees of freedom for the fit, the probability of seeing a χ^2 value that large or larger, and the estimated uncertainty in the weighted mean proper motion of the member stars in the x and y directions. The mean proper motion of the member stars is always much smaller than its uncertainty because that is forced by the fitting of the transformation.

TABLE 2. Information about Coordinate Transformations for CVn I

Field (1)	N_s (2)	N_m (3)	σ_a (pixel) (4)	N_f (5)	χ^2 (6)	N_{dof} (7)	$P(\chi^2)$ (8)	$\sigma_{\langle \mu \rangle, x}$ (10^{-3} pixel yr $^{-1}$) (9)	$\sigma_{\langle \mu \rangle, y}$ (10^{-3} pixel yr $^{-1}$) (10)
1s	559	535	0.0026	13	1018.57	1057	0.795	0.19	0.19
1t	349	338	0.0025	13	621.90	663	0.872	0.25	0.25
2s	80	73	0.0025	13	110.04	133	0.923	0.68	0.67
2t	46	36	0.0050	12	60.49	60	0.458	1.06	0.97
3s	158	141	0.0025	12	219.40	270	0.989	0.59	0.62
3t	172	161	0.0025	13	263.38	309	0.971	0.52	0.53
4s	276	266	0.0035	12	520.37	520	0.487	0.53	0.55
4t	237	227	0.0025	13	409.36	441	0.858	0.50	0.51

The raw motions in the frame moving with the galaxy are plotted versus S/N below, starting with Field 1. The left-hand set of four panels in each figure is for the s chip of the field and the right-hand set is for the t chip. Within the four-panel sets, the left-hand panels show stars accepted as members of the galaxy (with the QSO also shown as a star, if it is present), while the right-hand panels show objects with fitted proper motions (non-member stars – open circles, galaxies - filled triangles, and the QSO – a filled star).

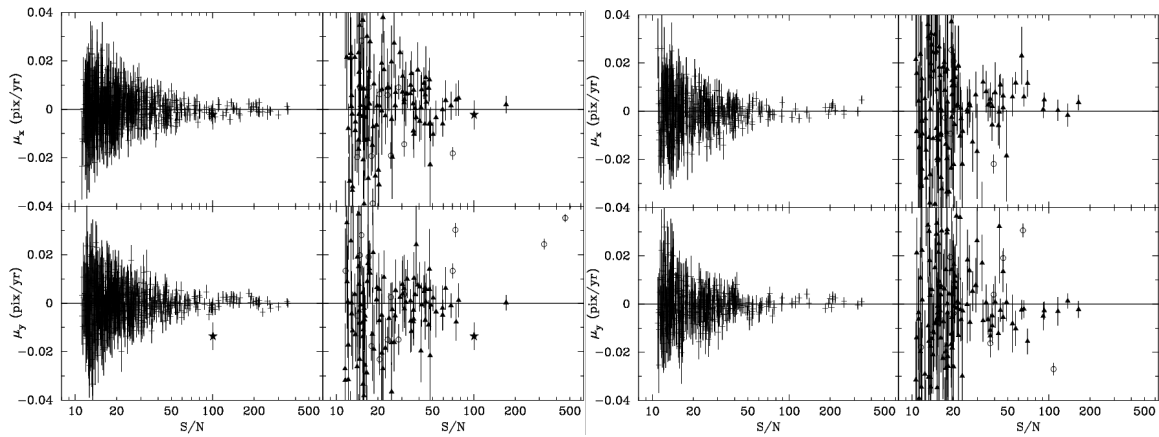


Figure 2. Raw motions vs. S/N for CVn I Field 1; chip s is to the left and chip t to the right. Plus symbols

are member stars, open circles are non-member stars, filled diamonds are galaxies, and the filled star is the QSO.

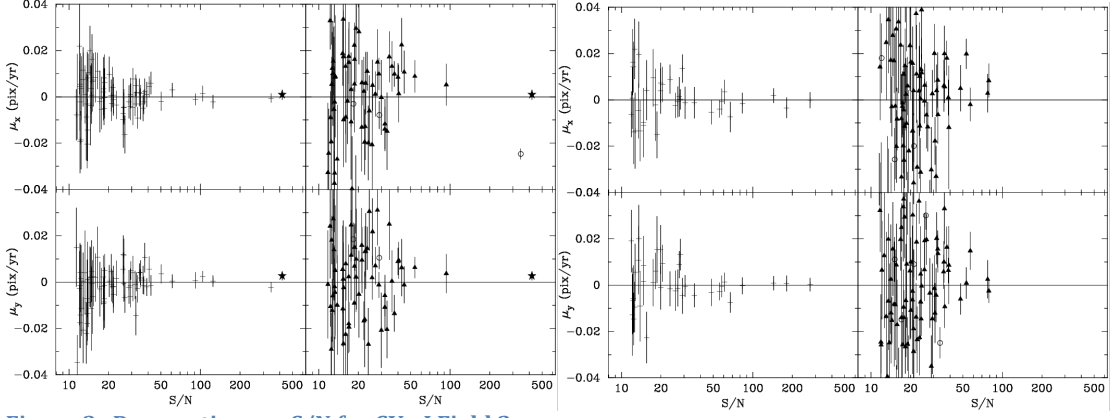


Figure 3. Raw motions vs S/N for CVn I Field 2.

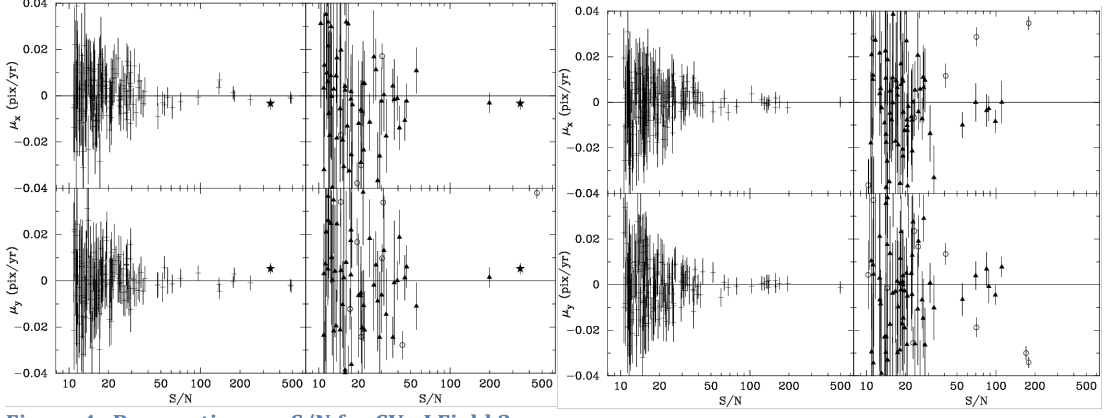


Figure 4. Raw motions vs S/N for CVn I Field 3.

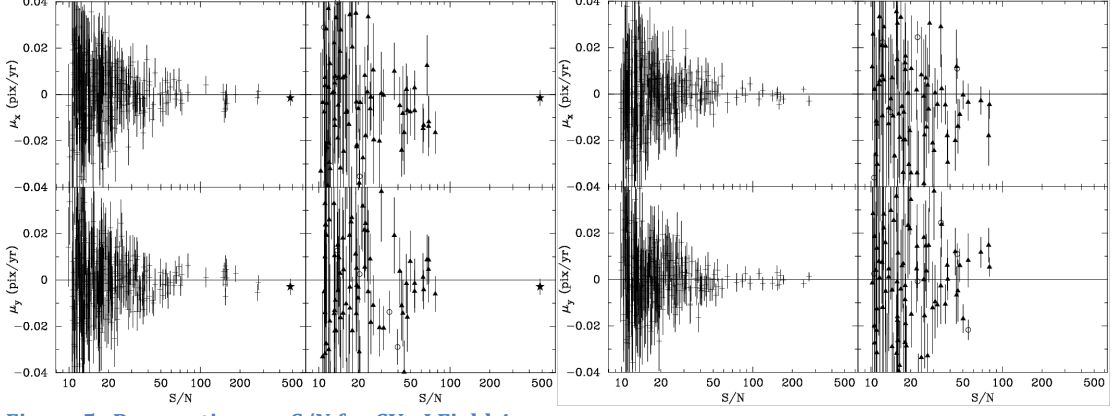


Figure 5. Raw motions vs S/N for CVn I Field 4.

The numbers of stars and galaxies in the various fields mirrors what is expected based on the placement of the fields with respect to the center of CVn I and the length of the exposure time. Because the proper motion of CVn I is small, the offset between the motion of the stars and the motion of the galaxies in the above plots is not readily apparent. Comparing the member and non-member stars in the plots shows that there is no ambiguity in assigning stars to the two groups.

To find the average motion of the galaxies in the coordinate frame moving with the stars of the galaxy, I used a program that calculates a weighted average of the galaxy motions. However, experience has shown that faint galaxies tend to show more scatter around the mean motion than is expected from the estimated uncertainties in their motions. These uncertainties are calculated from the uncertainties in the galaxy positions estimated from the scatter around the mean of the positions measured in different exposures. Thus, I group the galaxies into quartiles based on their S/N and find a single weighted mean, but also four uncertainty multipliers such that the overall chi-square of the scatter around the mean is one per degree of freedom. The results of this procedure are given in Table 3 below. N_g is the number of galaxies and (μ_x, μ_y) is the proper motion of CVn I (i.e., the negative of the mean galaxy motion). These are followed by the four multipliers (with the values for the x and y directions given separately) and the three S/N boundaries of the quartiles. For Fields 2, 3, and 4 a line also states the proper motion of CVn I based on using the QSO as a zero-point. This is not done from Field 1 since there the QSO is just another compact galaxy.

Raw proper motions from the two chips of a field can be compared directly since they have nearly the same orientation. The proper motion from the QSO and the galaxies in the s chip can also be compared directly. However, it is generally easier to convert the proper motions into (μ_α, μ_δ) using the orientation of the fields. The results of this are given in Table 4 and plotted in Figure 6.

TABLE 3. Information on Raw CVn I Proper Motions

Field	N_g	μ_x (10^{-3} pixel yr $^{-1}$)	μ_y	M_4	S/N	M_3	S/N	M_2	S/N	M_1
	(1)	(2)	(3)	(4)	x/y	(5)	x/y	(6)	x/y	x/y
1s	126	-1.67 ± 1.10	$+0.74 \pm 1.25$	2.61/2.95	14.6	1.81/2.53	18.4	1.29/1.85	34.9	1.09/1.10
1t	147	-3.10 ± 1.00	$+2.34 \pm 1.02$	1.90/2.04	13.6	2.20/1.82	17.0	1.75/2.04	22.1	1.07/1.04
2q	1	-0.93 ± 2.01	-2.64 ± 1.71							
2s	71	-6.14 ± 1.76	-1.43 ± 1.81	2.25/2.24	13.2	2.06/1.34	17.7	1.33/1.24	24.9	0.94/1.16
2t	86	-2.49 ± 2.39	-2.20 ± 2.10	1.76/1.68	16.0	2.39/2.53	20.1	1.28/1.75	26.8	1.66/1.39
3q	1	$+3.43 \pm 2.40$	-5.19 ± 2.24							
3s	69	$+2.67 \pm 1.91$	$+1.29 \pm 2.36$	2.59/2.73	12.2	1.37/2.22	15.9	1.35/1.76	21.9	0.88/0.98
3t	80	$+4.08 \pm 1.75$	-1.06 ± 2.20	1.56/1.79	13.9	0.77/1.60	17.8	1.31/1.08	22.4	1.03/1.35
4q	1	$+1.52 \pm 3.26$	$+2.91 \pm 3.34$							
4s	101	$+7.10 \pm 1.90$	$+3.64 \pm 2.52$	1.34/2.73	12.4	1.58/2.03	16.0	1.81/1.56	22.5	0.87/1.21
4t	90	$+5.08 \pm 1.85$	$+0.18 \pm 2.15$	1.78/1.33	12.9	2.18/1.44	16.7	1.59/1.26	25.8	0.91/1.32

The 11 individual measurements of the proper motion for CVn I agree with each other reasonably well. Multiplying all of the uncertainties by 1.12 produces a combined χ^2 for the scatter about the mean in both the α and δ directions of one per degree of freedom. The uncertainties listed in Table 5 and plotted in Figure 6 have been multiplied by this factor. The most discrepant measurement is for field 4s,

which is 2.1σ from the mean in μ_α . A lot of investigation has not revealed any reason for this field being discrepant.

TABLE 4. Measured Proper Motions
for CVn I

Field	Δt (yrs)	μ_α (mas century $^{-1}$)	μ_δ
(1)	(2)	(3)	(4)
1s	3.025	-4.4 ± 5.0	-5.8 ± 5.4
1t	"	-6.3 ± 4.5	-12.8 ± 4.8
2q	3.005	-10.6 ± 8.2	$+3.4 \pm 8.5$
2s	"	-19.3 ± 8.0	-16.1 ± 8.0
2t	"	-13.0 ± 10.8	-2.7 ± 11.2
3q	1.926	-1.0 ± 10.5	-24.7 ± 10.2
3s	"	-11.7 ± 9.1	-1.1 ± 10.0
3t	"	-11.7 ± 8.4	-12.0 ± 9.3
4q	1.902	-11.0 ± 14.2	$+7.1 \pm 16.6$
4s	"	-31.7 ± 9.2	-1.5 ± 10.6
4t	"	-17.9 ± 8.6	-9.4 ± 9.3
mean		-12.5 ± 2.5	-8.6 ± 2.4

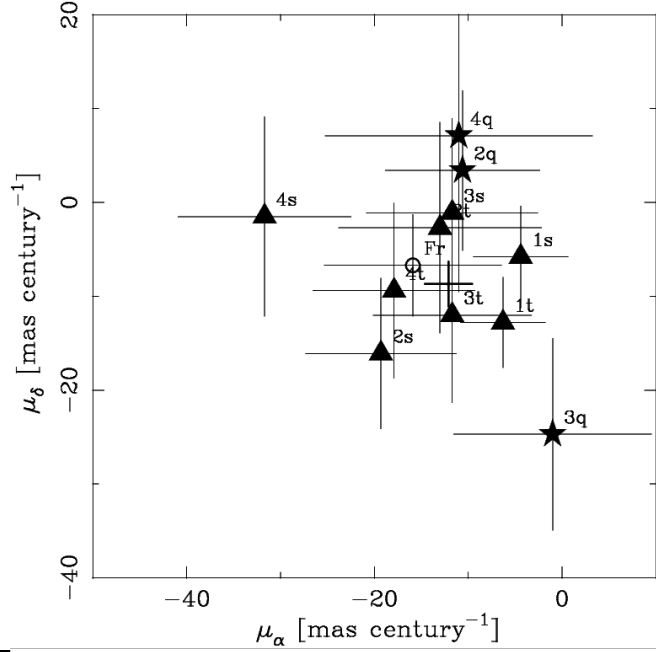


Figure 6. Proper motion measurements for CVn I. Also shown as an open circle is the measurement by Fritz et al. (2018).

Also plotted in Figure 10 is the measurement using Gaia DR2 data from Fritz, *et al.* (2018) of $(\mu_\alpha, \mu_\delta) = (-15.9 \pm 9.4, -6.7 \pm 5.4)$ mas century $^{-1}$. The agreement between this value and our mean is good.

Coma Bernices (I): This galaxy is at moderately high galactic latitude $(l, b) = (241.9^\circ, +83.6^\circ)$ and has a distance from the Sun of 44 ± 4 kpc (McConnachie 2012). With an M_V of -4.1 , it is clearly among the group of nearby ultra-faint satellite galaxies found in the SDSS. It has a heliocentric radial velocity of 98.1 ± 0.9 km/s (Simon & Geha 2007).

We have two fields in this galaxy, which are shown in the figure below. Field 1 is the more northerly of the two.

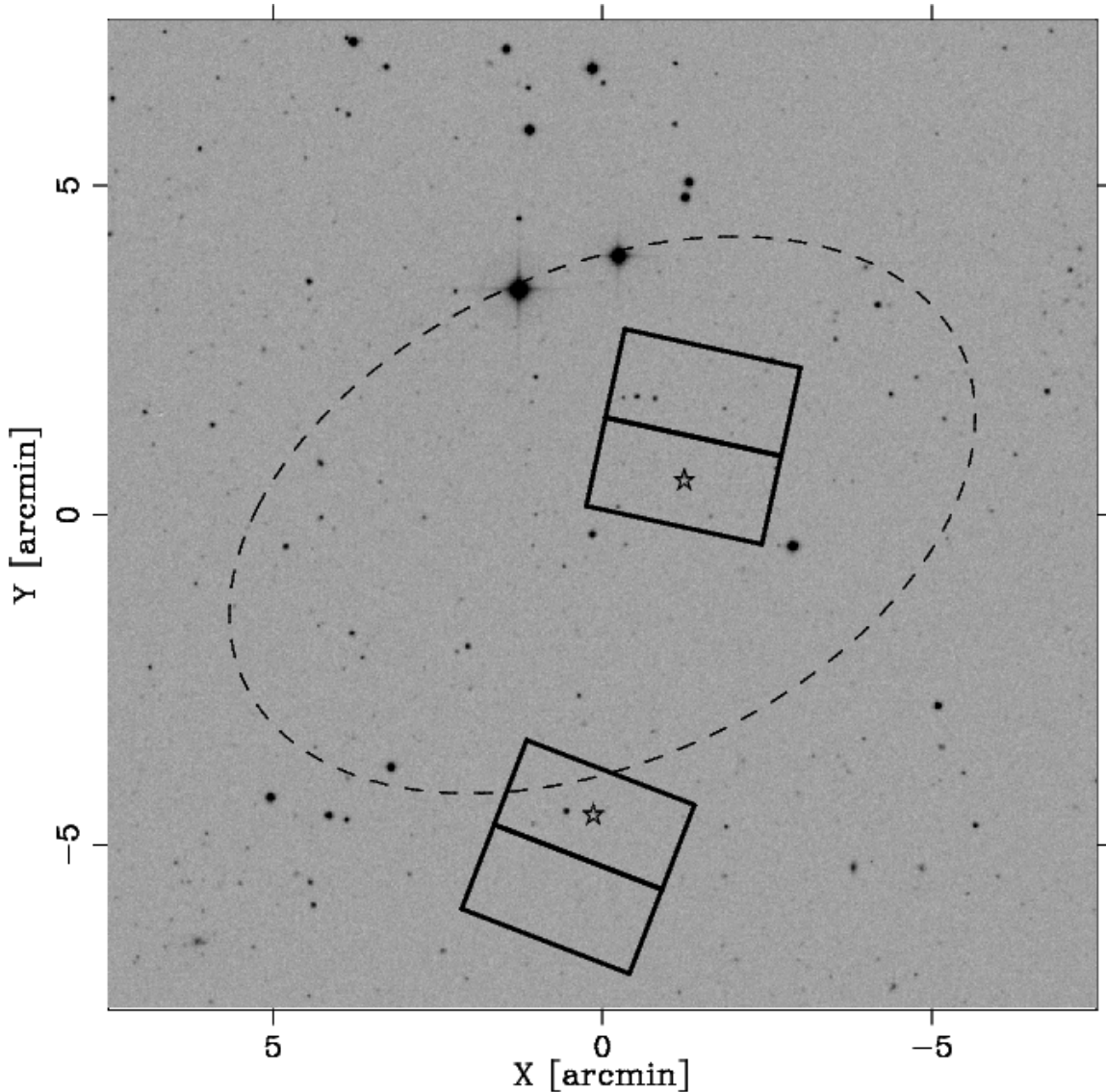


Figure 7. Fields for Coma galaxy. Field 1 is the more northerly of the two. The dashed ellipse is the half-light radius.

We have three epochs of data for Coma, as shown in Table 5. All of the images are reduced and we have used the average PSF from all three epochs to measure the positions of the stars and galaxies. However, only the first and last epoch have been used to measure the proper motion.

TABLE 5. Information about Coma Pointings and Images

Pointing (1)	R.A. (J2000.0) (2)	Decl. (J2000.0) (3)	Date yyyy – mm – dd (4)	(X_Q, Y_Q) (pix, pix) (5)	PA (deg.) (6)	T_{exp} (s) (7)
Coma-1	12:26:53.6	+23:54:58.5	2010 – 12 – 01	(2033.07, 1005.15)	168	$5 \times 480, 10 \times 503$
			2011 – 12 – 23	(2034.06, 1002.71)	168	$5 \times 474, 10 \times 496$
			2013 – 01 – 03	(2033.45, 1002.92)	168	$5 \times 474, 10 \times 496$
Coma-2	12:26:59.6	+23:49:54.4	2010 – 06 – 21	(2032.14, 1013.19)	-21	$5 \times 480, 10 \times 503$
			2011 – 06 – 05	(2032.86, 1013.69)	-21	$5 \times 474, 10 \times 496$
			2012 – 05 – 13	(2033.61, 1011.78)	-21	$5 \times 474, 10 \times 496$

The raw motions in the frame moving with Coma are plotted versus S/N in the figures below. The left-hand set of four panels in each figure is for the s chip of the field and the right-hand set is for the t chip. Note that the vertical range is more than twice as large as for the equivalent plots for CVn I in order to show the galaxies, which are clearly offset from the stars.

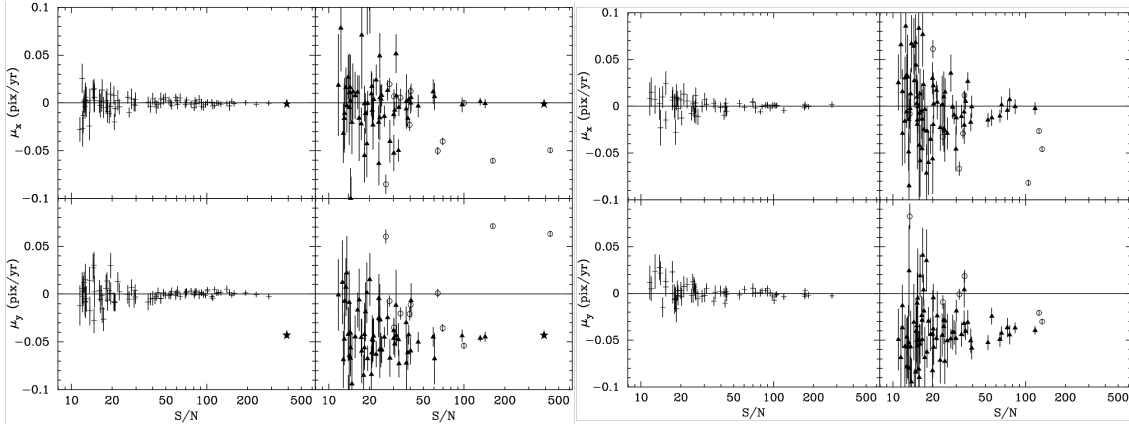


Figure 8. Raw motions vs S/N for the Coma 1 field. Chip s is to the left and chip t to the right. Plus symbols are member stars, open circles are non-member stars, filled diamonds are galaxies, and the filled star is the QSO.

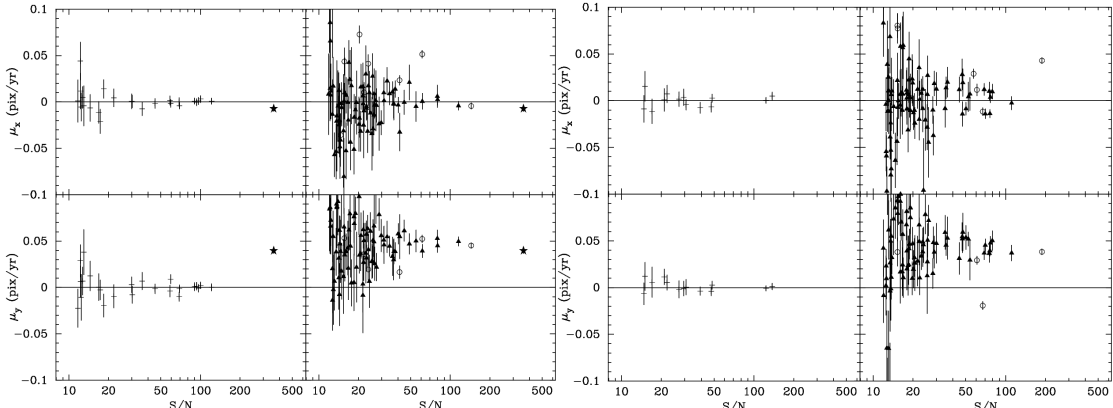


Figure 9. Raw motions vs S/N for the Coma 2 field. Chip s is to the left and chip t to the right.

In the Coma 1s field there is a star with a S/N of 100 that has a motion consistent with that of the galaxies and inconsistent with that of the member stars. I examined the image of this object and there is nothing in its profile or surroundings to suggest that it is not a star. This object is probably a QSO, but in the absence of spectroscopic evidence I left it as a (non-member) star. There are similar objects with a S/N of 144 in the Coma 2s field and 61 in the Coma 2t field. These have stellar widths and no adjacent “fuzz” of light. The object in Coma 2s maybe is connected to nearby galaxies by faint light bridges, but this field has lots of galaxies in it so this is not definitive. Again, these objects are likely QSOs. I decided to include the Coma 2s object in the galaxy sample (using its motion measured by treating it is a star; which also means keeping its contribution to the stellar PSF), but left the other objects as non-member stars. The resulting change in the raw motion derived from the 2s field was about 0.7σ in x direction and 0.4σ in the y direction, making the agreement with the other measurements slightly better.

TABLE 6. Information about Coordinate Transformations for Coma

Fi-eld (1)	N_s (2)	N_m (3)	σ_a (pixel) (4)	N_f (5)	χ^2 (6)	N_{dof} (7)	$P(\chi^2)$ (8)	$\sigma_{\langle \mu \rangle, x}$ (10^{-3} pixel yr $^{-1}$) (9)	$\sigma_{\langle \mu \rangle, y}$ (10^{-3} pixel yr $^{-1}$) (10)
1s	96	81	0.0025	13	122.96	149	0.941	0.46	0.47
1t	71	62	0.0026	12	112.15	112	0.478	0.55	0.58
2s	35	24	0.0032	12	35.90	36	0.473	1.13	1.28
2t	20	13	0.0025	12	13.80	14	0.465	1.63	1.48

Even the nearly centrally-positioned Field 1 does not have many stars in it, a reflection of the low luminosity and low surface brightness of Coma. The very small number of members stars in Field 2t is a concern. However, I tried different numbers of terms in the transformation all of the way down to just 6 and the proper motion did not change significantly.

Averaging the galaxies in the different fields produced the results in Table 7. The large y motion of Coma is apparent.

TABLE 7. Information on Raw Coma Proper Motions

Fi-eld (1)	N_g (2)	μ_x (10^{-3} pixel yr $^{-1}$) (3)	μ_y (4)	M_4 (5)	S/N x/y (6)	M_3 (7)	S/N x/y (8)	M_2 (9)	S/N x/y (10)	M_1 (11)
1q	1	$+1.09 \pm 2.23$	$+43.09 \pm 2.67$							
1s	66	$+2.49 \pm 2.39$	$+45.96 \pm 1.66$	1.90/2.89	14.8	1.95/1.61	21.0	1.41/0.85	31.1	1.37/0.93
1t	76	$+3.18 \pm 2.10$	$+39.50 \pm 1.86$	1.68/2.37	14.6	1.21/1.33	17.6	1.45/1.12	27.8	1.13/1.06
2q	1	$+7.18 \pm 2.99$	-39.61 ± 2.88							
2s	87	$+1.58 \pm 1.47$	-46.88 ± 1.43	1.52/1.91	14.4	1.30/1.19	19.8	0.76/0.89	26.9	0.89/0.87
2t	85	$+1.14 \pm 2.04$	-43.92 ± 1.64	1.76/1.68	16.0	2.39/2.53	20.1	1.28/1.75	26.8	1.66/1.39

Converting the raw motions into proper motions yields the results in Table 8. The uncertainties in the zero-point of the stellar reference frame are not negligible compared to the uncertainty from the mean galaxy motion for Field 2. Thus, the two uncertainties were added in quadrature for both fields before converting to (μ_α, μ_δ) . The scatter of the individual measurements around their mean was slightly larger than expected from the uncertainties. Multiplying the uncertainties by 1.23 produced a χ^2 per degree of freedom of one for μ_α and μ_δ combined. The uncertainties listed in Table 8 and plotted in Figure 10 have been multiplied by that factor. Also plotted in Figure 10 is the measurement using Gaia DR2 data from Simon (2018) of $(\mu_\alpha, \mu_\delta) = (+54.6 \pm 9.2, -172.6 \pm 8.6)$ mas century $^{-1}$. The agreement between this value and our mean is good.

TABLE 8. Measured Proper Motions for Coma

Field (1)	Δt (yrs) (2)	μ_α (mas century $^{-1}$) (3)	μ_δ (mas century $^{-1}$) (4)
1q	2.092	$+40.7 \pm 11.2$	-166.5 ± 13.2
1s	"	$+48.6 \pm 11.8$	-176.5 ± 8.6
1t	"	$+46.0 \pm 10.6$	-150.8 ± 9.6
2q	1.893	$+29.9 \pm 15.6$	-157.3 ± 15.5
2s	"	$+61.1 \pm 9.1$	-176.3 ± 9.3
2t	"	$+58.5 \pm 12.5$	-164.7 ± 11.1
mean		$+49.7 \pm 4.6$	-166.9 ± 4.3

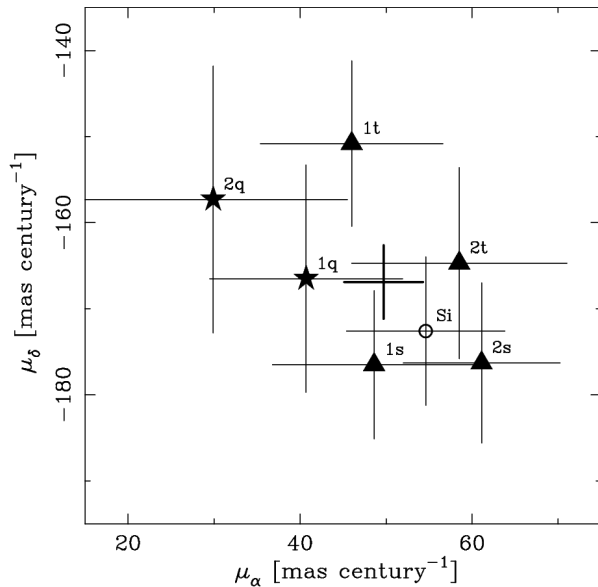


Figure 10. Proper motion measurements for Coma. Also shown as an open circle is the measurement by Simon (2018).

Bootes I: This galaxy is at galactic latitude $(l, b) = (358.1^\circ, +69.6^\circ)$ and has a distance from the Sun of 66 ± 2 kpc (McConnachie 2012). With an M_V of -6.3 , it is among the more luminous of the group of nearby ultra-faint satellite galaxies found in the SDSS. It has a heliocentric radial velocity of 101.8 ± 0.7 km/s (Koposov et al. 2011).

We have two fields in this galaxy, which are shown in Figure 11 below. Field 1 is the more northerly of the two.

We have three epochs of data for Boo I, as shown in Table 9. All of the images are reduced and we have used the average PSF from all three epochs to measure the positions of the stars and galaxies. However, only the first and last epoch have been used to measure the proper motion. The QSO in Field 1 has $V=20.60$ and that in Field 2 has $V=20.05$, which is the reason for the shorter exposure times in Field 2.

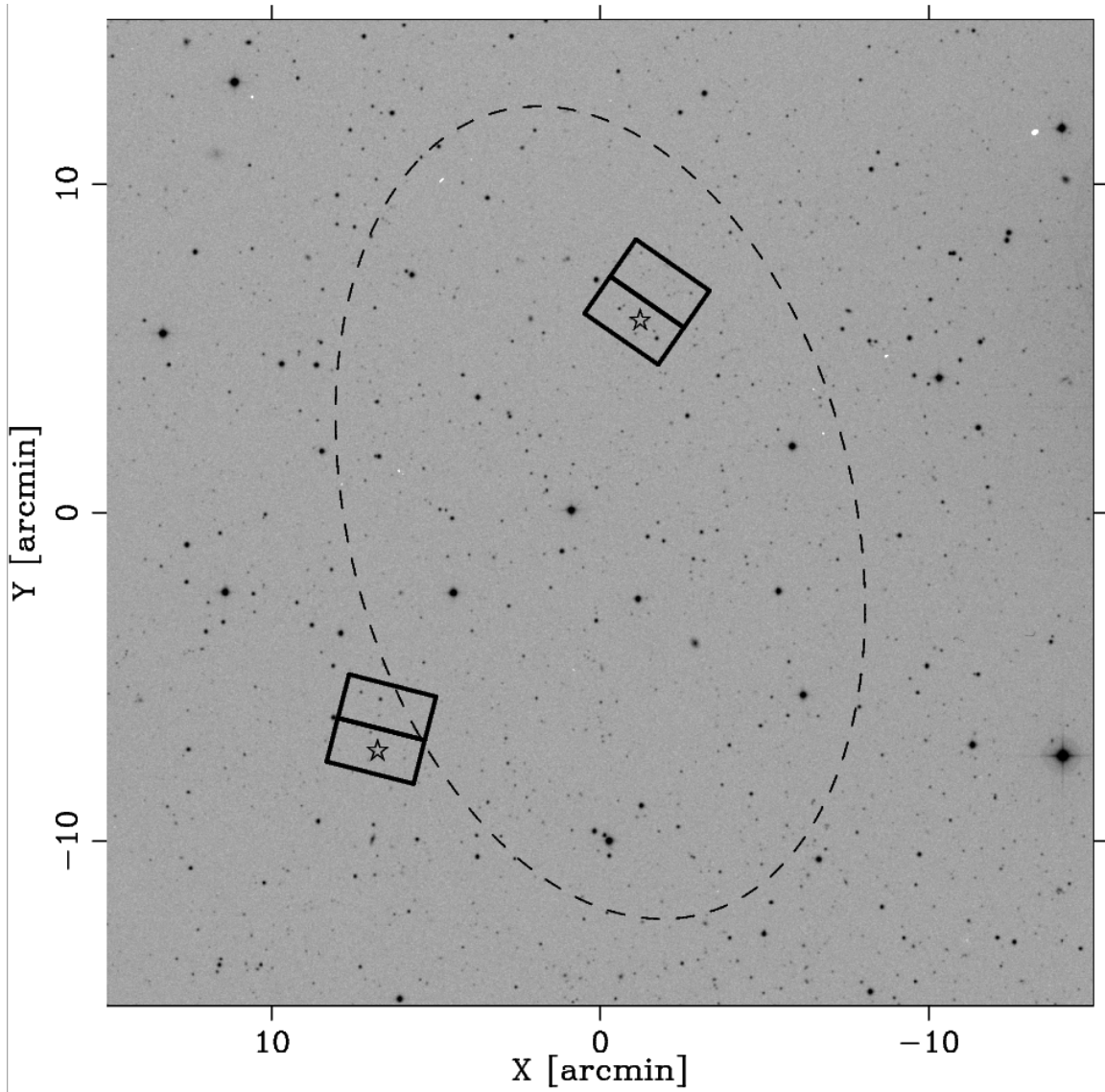


Figure 11. The position of the two fields observed in Bootes I. The more northerly on the two is Field 1.

TABLE 9. Information about Boo I Pointings and Images

Pointing (1)	R.A. (J2000.0) (2)	Decl. (J2000.0) (3)	Date yyyy – mm – dd (4)	(X_Q, Y_Q) (pix, pix) (5)	PA (deg.) (6)	T_{exp} (s) (7)
Boo I-1	13:59:59.7	+14:36:33.2	2011 – 01 – 14	(2026.33, 1020.32)	145	$4 \times 631, 8 \times 659$
			2012 – 02 – 05	(2031.58, 1012.01)	145	12×625
			2013 – 02 – 23	(2026.00, 1007.24)	145	12×625
Boo I-2	14:00:32.2	+14:23:27.3	2009 – 12 – 24	(2028.46, 1018.79)	166	$6 \times 378, 12 \times 396$
			2011 – 01 – 20	(2031.52, 1014.17)	166	$6 \times 377, 12 \times 395$
			2012 – 12 – 27	(2032.27, 1012.96)	166	$6 \times 372, 12 \times 390$

The raw motions in the frame moving with Boo I are plotted versus S/N in the figures below. Note that the vertical range is 50% larger than for the equivalent plots for CVn I in order to show the galaxies, which are clearly offset from the member stars.

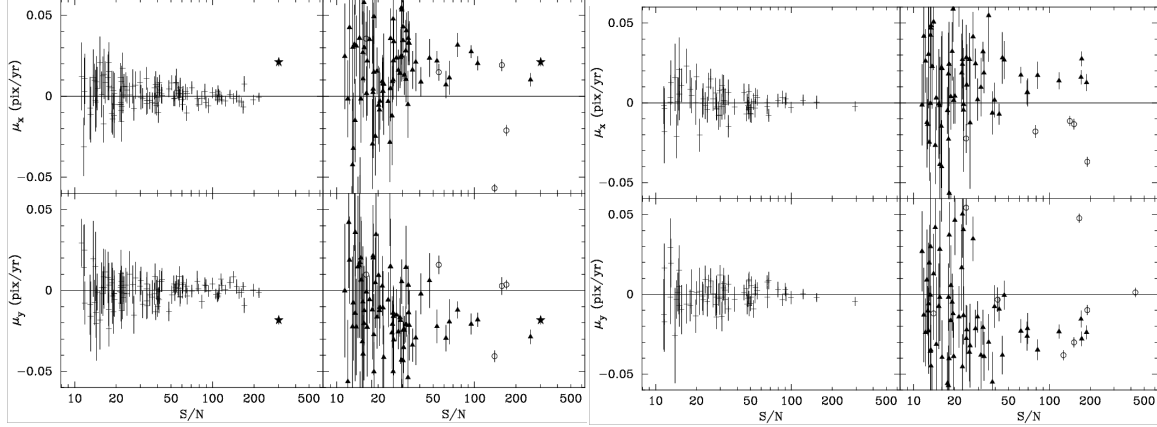


Figure 12. Raw motions vs S/N in Boo I Field 1. Chip s is to the left and chip t to the right. Plus symbols are member stars, open circles are non-member stars, filled diamonds are galaxies, and the filled star is the QSO.

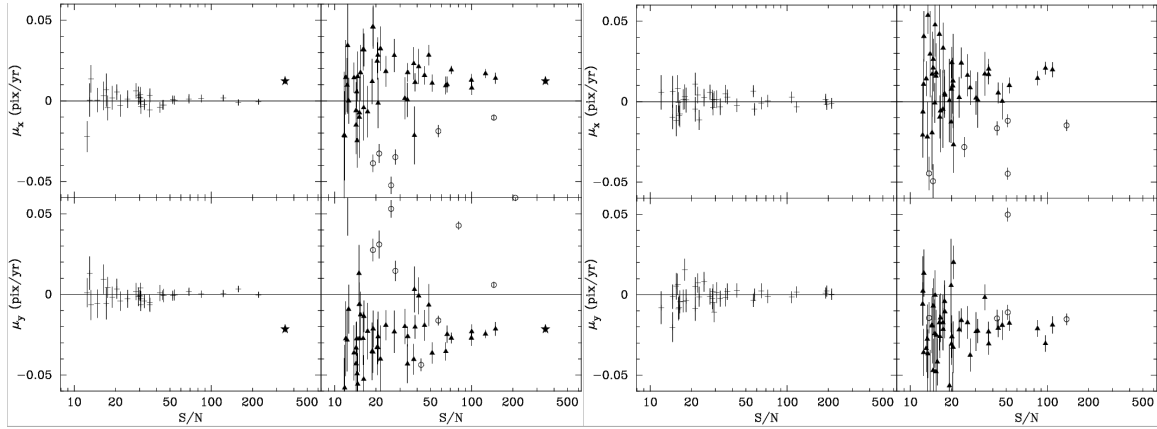


Figure 13. Raw motions vs S/N in Boo I Field 2. Chip s is to the left and chip t to the right.

The large offset between the member stars and galaxies allowed some further investigation of the status of some objects. In Field 1s, two relatively bright objects that we had classified as galaxies, object 200 at (1547.19, 974.41) with S/N=161.5 and object 201 at (3913.81, 1025.41) with S/N=77.4, had motions indicating that they were member stars. They are clearly associated with galaxies in the images, but examination suggested that they are bright stars superimposed on faint galaxies. So I turned them into stars. There were also two objects in Field 1s that were originally classified as stars, but have motions indicating that they are galaxies. Object 5501, at (3533.43, 1118.56) with S/N=28.6, looks very stellar but has a profile that is maybe slightly extended. Object 5502, at (2379.85, 673.75) with S/N=94.6, has a stellar profile, but has some arcs (gravitational lensing?) and faint background light around it. I made both of these galaxies. Then I reran the gpf

program scripts. Field 1t did not have any objects that seemed likely to be misclassified. There are 20 stars with large proper motions in this field, whereas there are only 5 in the 1s field. It is curious that there is this difference when the two fields are so close together. The stars are not clumped in proper motion (well, no more than a few of them anyway), so this does not appear to be a stellar stream. The two vector point plots of the raw motions are below (note the different scales).

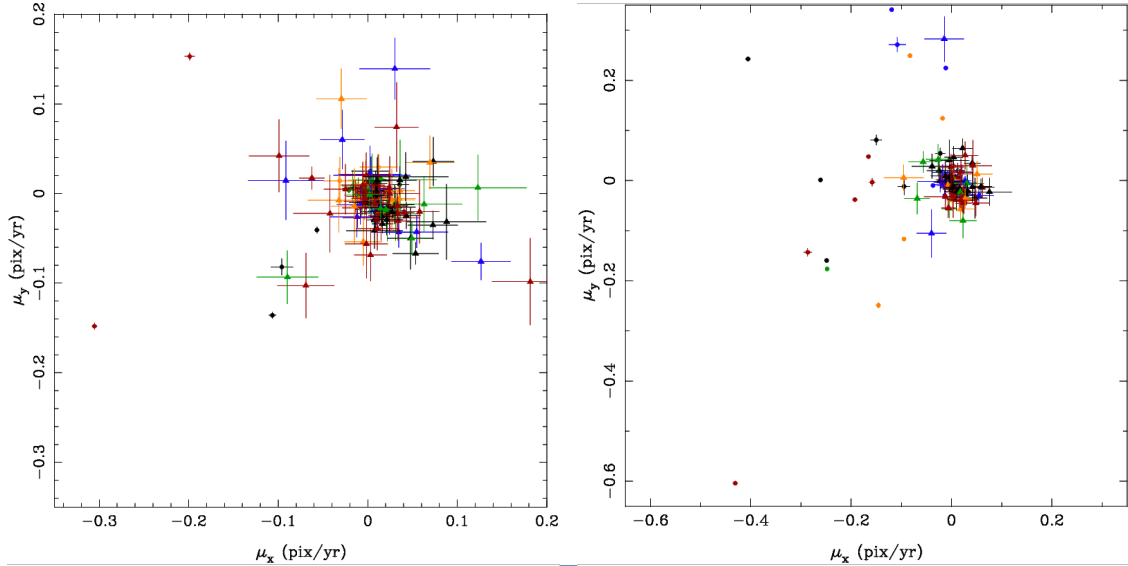


Figure 14. Vector point plots for the raw motions in the Boo I fields 1s (left) and 1t (right). Filled circles are (non-member) stars and filled triangles are galaxies. The different colors indicate location on the chips.

In Field 2s there was one object that was originally classified as stellar that appears to have a galaxy motion, 5400 at (3123.16, 587.39) with a S/N of 71.1. It is about 20 pixels from a faint galaxy, but its profile is stellar and there is no fuzz around it. If I were being consistent with Coma I would have kept it a star, but I turned it into a galaxy. There were no objects in Field 2t that needed to have their type changed.

TABLE 10. Information about Coordinate Transformations for Boo I

Field (1)	N _s (2)	N _m (3)	σ_a (pixel) (4)	N _f (5)	χ^2 (6)	N _{dof} (7)	P(χ^2) (8)	$\sigma_{(\mu),x}$ (10^{-3} pixel yr ⁻¹) (9)	$\sigma_{(\mu),y}$ (10)
1s	118	109	0.0025	12	187.51	206	0.818	0.49	0.51
1t	89	68	0.0032	12	124.15	124	0.479	0.71	0.72
2s	44	31	0.0025	12	44.05	50	0.710	0.57	0.60
2t	46	35	0.0065	12	57.72	58	0.486	0.80	0.83

Table 10 shows that Field 2t required a larger-than-usual additional uncertainty to produce a χ^2 of one per degree of freedom for the transformation between epochs. The reason is not obvious. Dividing the sample into bright and faint stars at S/N = 25 shows that fainter stars provide a disproportionate amount of the χ^2 . Figure 13

shows that this field does have a few bright stars with motions close to those of the member stars but still classified as non-members. No amount of fiddling with the transformation made these stars members. These stars are somewhat clumped in proper motion and there are one or two faint stars with similar motions, but which were classified as members. It is possible that these stars, which cannot be clearly distinguished from the member stars because of their larger motion uncertainties, are what is requiring the larger additional uncertainty. Though in that case it is somewhat surprising that the adjacent Field 2s is not affected in the same way. The vector point plots of the motions for Fields 2s and 2t, expanded around (0,0) are shown below. Well, excluding the two lower-S/N stars closest to the clump of brighter stars (52 and 82) only allowed the additional uncertainty to be lowered to 0.0052. So this explanation does not seem very convincing and the origin of the larger additional uncertainty remains unexplained.

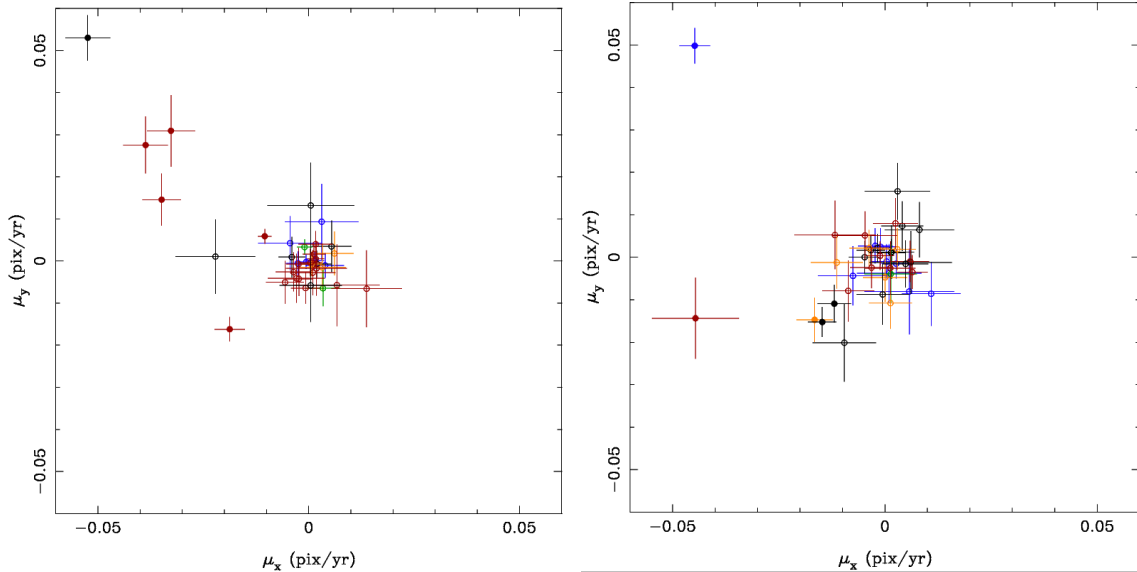


Figure 15. Vector point plot showing stars for Fields 2s (left) and 2t (right), expanded around (0,0).
Members are filled circles and non-members are open.

Averaging the galaxy motions in the different fields produced the results in Table 11. The large motion of Boo I is apparent.

TABLE 11. Information on Raw Boo I Proper Motions

Fi- eld (1)	N _g (2)	μ_x (10 ⁻³ pixel yr ⁻¹) (3)	μ_y (4)	M ₄ x/y (5)	S/N 4,3 (6)	M ₃ x/y (7)	S/N 3,2 (8)	M ₂ x/y (9)	S/N 2,1 (10)	M ₁ x/y (11)
1q	1	-21.02 ± 2.30	$+18.38 \pm 2.34$							
1s	83	-19.40 ± 1.71	$+19.50 \pm 1.81$	2.34/1.78	15.4	1.29/1.39	21.5	0.97/1.38	30.3	1.22/1.12
1t	65	-15.44 ± 2.12	$+21.10 \pm 1.94$	1.39/1.13	14.5	1.27/2.43	19.4	1.26/1.63	30.5	1.52/1.24
2q	1	-12.25 ± 1.71	$+21.61 \pm 1.61$							
2s	46	-14.95 ± 1.16	$+25.29 \pm 1.29$	1.17/1.29	14.7	1.68/1.17	19.8	1.17/1.00	38.5	1.14/1.16
2t	47	-14.65 ± 1.54	$+20.48 \pm 1.66$	1.96/1.24	14.5	1.28/0.83	17.6	1.12/1.55	26.7	1.01/1.15

Converting the raw motions into proper motions yields the results in Table 12. The uncertainties in the zero-point of the stellar reference frame are not entirely negligible compared to the uncertainty from the mean galaxy motion. Thus, the two uncertainties were added in quadrature for both fields before converting to (μ_α, μ_δ) .

TABLE 12. Measured Proper Motions for Boo I

Field	Δt (yrs)	μ_α (mas century $^{-1}$)	μ_δ (mas century $^{-1}$)
(1)	(2)	(3)	(4)
1q	2.109	-26.9 ± 12.8	-107.7 ± 12.9
1s	"	-19.1 ± 9.8	-107.7 ± 9.9
1t	"	-2.4 ± 11.8	-104.0 ± 11.6
2q	3.009	-25.9 ± 9.7	-95.3 ± 9.4
2s	"	-32.7 ± 7.1	-112.2 ± 7.6
2t	"	-36.2 ± 9.4	-93.4 ± 9.9
mean		-26.2 ± 3.9	-103.9 ± 4.0

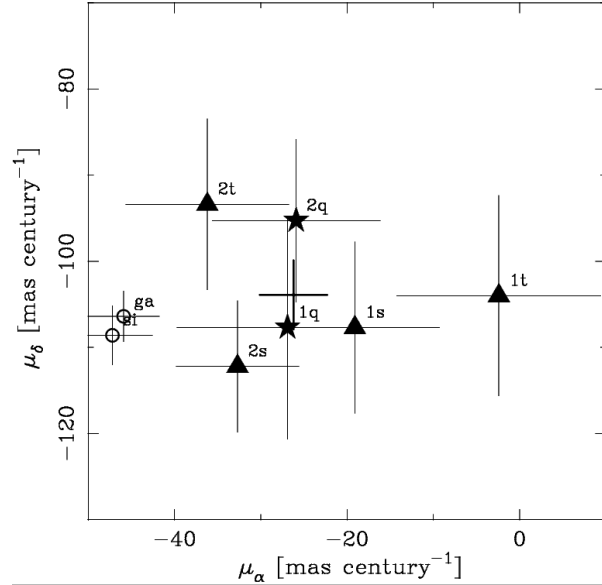


Figure 16. Proper motion measurements for Boo I. Also shown as an open circle is the measurement by Simon (2018) and the Gaia Collaboration (2018).

The scatter of the individual measurements around their mean was slightly larger than expected from the uncertainties. Multiplying the uncertainties by 1.36 produced a χ^2 per degree of freedom of one for μ_α and μ_δ combined. The uncertainties listed in Table 12 and plotted in Figure 16 have been multiplied by that factor.

Also plotted in Figure 16 are the measurements using the Gaia DR2 data from both the Gaia Collaboration (2018) of $(\mu_\alpha, \mu_\delta) = (-45.9 \pm 4.1, -106.4 \pm 2.9)$ mas century $^{-1}$ and from Simon (2018) of $(\mu_\alpha, \mu_\delta) = -47.2 \pm 4.6, -108.6 \pm 3.4$ mas century $^{-1}$. The agreement between these values and our mean is poor in right ascension. For example our μ_α and that of the Gaia Collaboration differ by 19.7 ± 5.7 mas century $^{-1}$, which is a difference of 3.5σ . At the distance of Boo I this corresponds to a difference in tangential velocity of 62 km s $^{-1}$. The disagreement is surprising given the good agreement between the two measurements for Coma. I currently do not see any reason for the difference.

I downloaded the Gaia DR2 stars in the direction of our Boo I fields and matched them with our samples. Most of our sample is below the DR2 limiting magnitude and many of the brighter DR2 stars in our fields are saturated in our images.

There were just 4 stars in our Boo I 1s field sample that were bright enough to be in the DR2 sample and, of these, three were saturated in our images and the last was too faint to have a solution for parallax and proper motion in DR2.

In the Boo I 1t sample there were 7 stars bright enough to be in DR2, but three were saturated in our images and two were too faint to have a solution for parallax and proper motion in DR2. The other two had the following proper motions.

$$\text{star 16: DR2 } (\mu_\alpha, \mu_\delta) = (+389 \pm 131, -1575 \pm 108) \text{ mas century}^{-1};$$

$$\text{us} = (+360 \pm 12, -1488 \pm 12) \text{ mas century}^{-1}$$

$$\text{star 62: DR2 } (\mu_\alpha, \mu_\delta) = (-722 \pm 119, -745 \pm 93) \text{ mas century}^{-1};$$

$$\text{us} = (-876 \pm 12, -702 \pm 12) \text{ mas century}^{-1}$$

There were just 3 stars in our Boo I 2s field sample that were bright enough to be in the DR2 sample and, of these, one was saturated in our images and the other two (the QSO and star 28) have large proper motion uncertainties —

$$\text{QSO: DR2 } (\mu_\alpha, \mu_\delta) = (+258 \pm 211, -281 \pm 183) \text{ mas century}^{-1};$$

$$\text{us} = (+11 \pm 11, -21 \pm 11) \text{ mas century}^{-1}$$

$$\text{star 28: DR2 } (\mu_\alpha, \mu_\delta) = (-562 \pm 209, -1099 \pm 229) \text{ mas century}^{-1};$$

$$\text{us} = (-529.7 \pm 8.1, -1097.5 \pm 7.8) \text{ mas century}^{-1}.$$

Finally, there were 3 stars in common with our Boo I 2t field, of which two were saturated in our images and the third has the following proper motion

$$\text{star 67: DR2 } (\mu_\alpha, \mu_\delta) = (-379 \pm 67, -533 \pm 47) \text{ mas century}^{-1};$$

$$\text{us} = (-304 \pm 13, -552 \pm 13) \text{ mas century}^{-1}.$$

Thus, agreement between the DR2 proper motions and our measurements is good, but the uncertainties are large enough in the DR2 that these data can't cast any light on a difference of

$$(\mu_{\alpha,\text{Gaia}} - \mu_{\alpha,\text{us}}, \mu_{\delta,\text{Gaia}} - \mu_{\delta,\text{us}}) = (-19.7 \pm 5.7, -2.5 \pm 4.9) \text{ mas century}^{-1}.$$

The weighted mean difference between the measurements for the 5 objects is

$$(\mu_{\alpha,\text{Gaia}} - \mu_{\alpha,\text{us}}, \mu_{\delta,\text{Gaia}} - \mu_{\delta,\text{us}}) = +3 \pm 51, -18 \pm 39 \text{ mas century}^{-1}.$$

Ursa Majoris I: This galaxy is at galactic latitude $(l,b) = (159.4^\circ, +54.4^\circ)$ and has a distance from the Sun of 97 ± 4 kpc (McConnachie 2012). With an M_V of -5.5 , it is a typical member of the group of ultra-faint satellite galaxies found in the SDSS. It has a heliocentric radial velocity of -55.3 ± 1.4 (Simon & Geha 2007).

We have two fields in this galaxy, which are shown in Figure 17 below. Field 1 is the more northerly of the two.

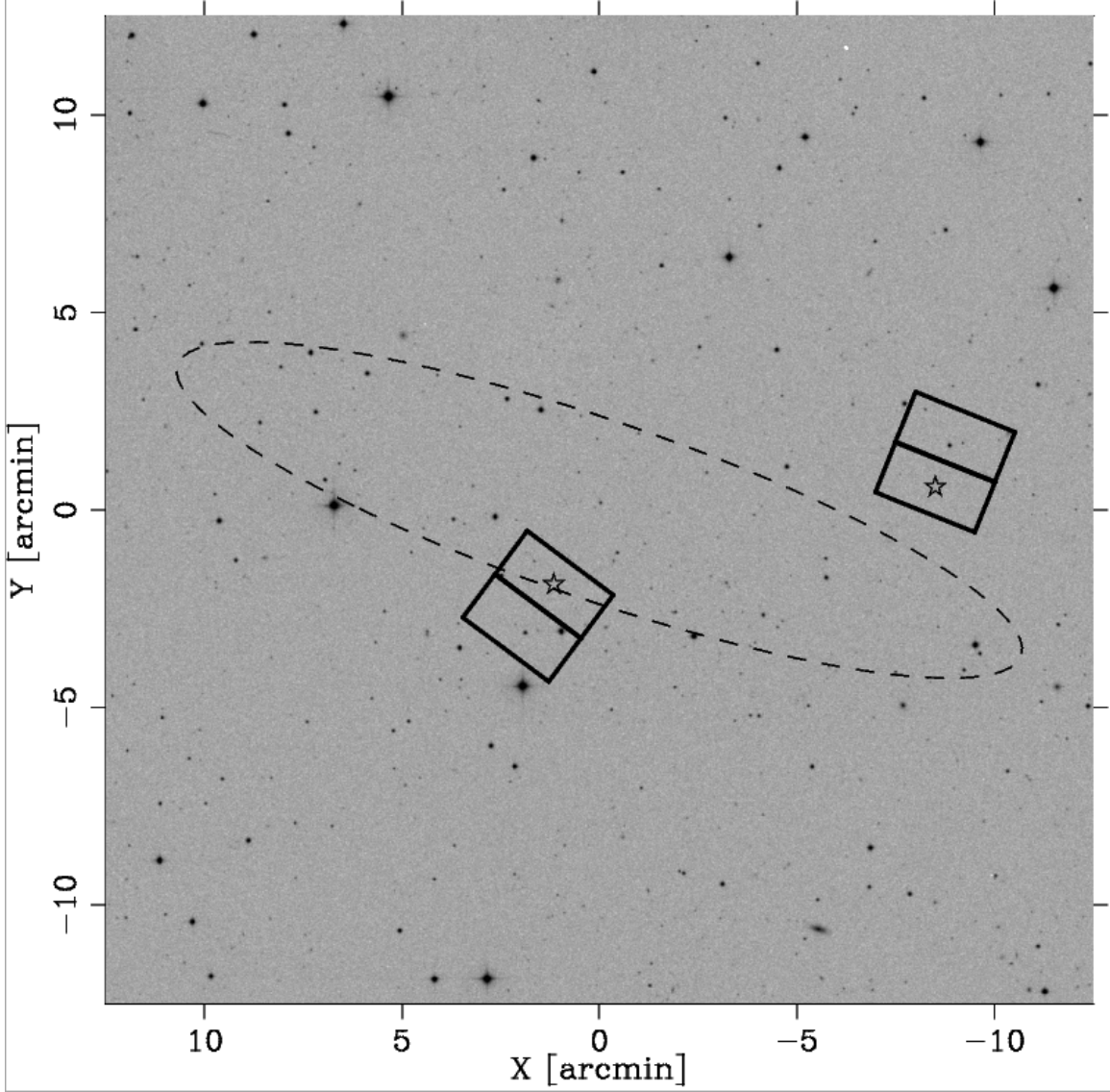


Figure 17. The position of the two fields observed in UMa I. The more northerly of the two is Field 1.

We have two epochs of data for UMa I, as shown in Table 13. Exposure times for the individual images are relatively long. The two pointing are oriented approximately 180° to each other.

TABLE 13. Information about UMa I Pointings and Images

Pointing (1)	R.A. (J2000.0) (2)	Decl. (J2000.0) (3)	Date yyyy – mm – dd (4)	(X_Q, Y_Q) (pix, pix) (5)	PA (deg.) (6)	T_{exp} (s) (7)
UMa I-1	10:33:53.8	+51:56:40.0	2009 – 11 – 18 2012 – 11 – 14	(2039.09, 1033.92) (2043.61, 1029.31)	158	$4 \times 682,8 \times 709$ $4 \times 671,8 \times 699$
UMa I-2	10:34:56.5	+51:54:12.9	2010 – 06 – 09 2012 – 06 – 02	(2040.25, 1021.56) (2041.22, 1020.18)	-37	$4 \times 682,8 \times 709$ $4 \times 675,8 \times 702$

The raw motions in the frame moving with UMa I are plotted versus S/N in the figures below. Note that the vertical range is 25% larger than for the equivalent plots for CVn I in order to show the galaxies, which are clearly offset from the member stars.

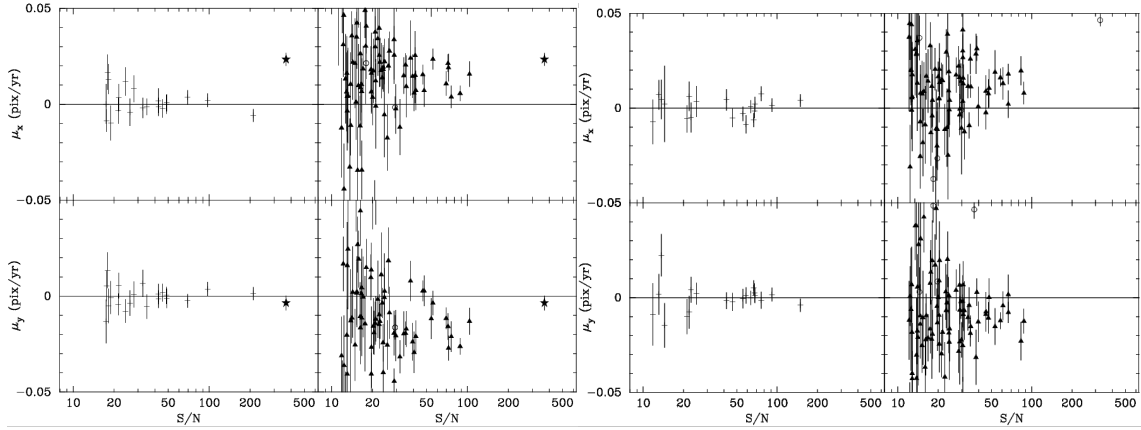


Figure 18. Raw motions vs S/N for UMa I Field 1. Chip s is to the left and chip t to the right. Plus symbols are member stars, open circles are non-member stars, filled diamonds are galaxies, and the filled star is the QSO.

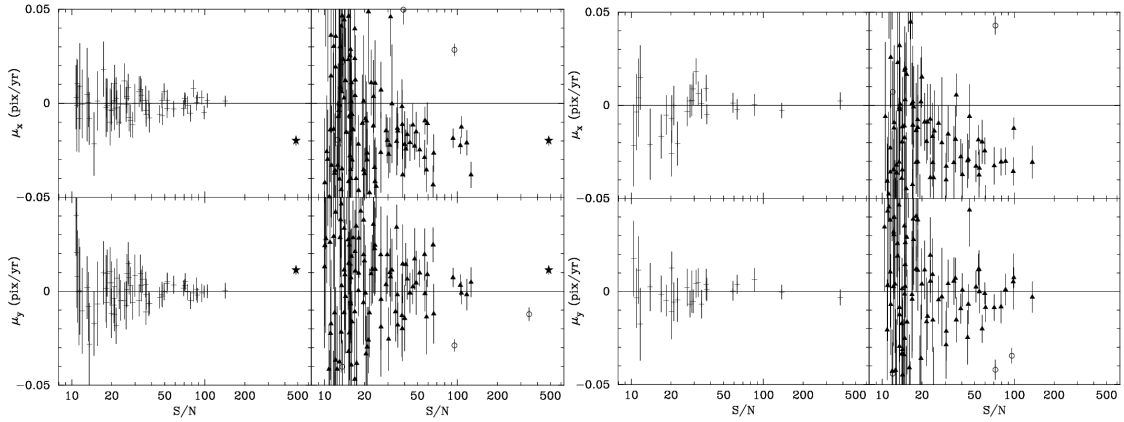


Figure 19. Raw motions vs S/N for UMa I Field 2. Chip s is to the left and chip t to the right.

There are clearly very few stars in all of the fields except for Field 2s. I plotted the members and non-member stars in Fields 2s and 2t. The number of member stars in the bottom two quadrants of Field 2s (14 and 11) are about 60% of those in the top two quadrants (22 and 17), with a smaller, though noticeable, gradient from the left to the right quadrants. The number of member stars in the quadrants of Field 2t are about half of the number the bottom quadrants of Field 2s (7 and 5 in the top two quadrants and 4 and 7 in the bottom two). Non-member stars are nearly equally spread over all of the quadrants of both fields (about 2 per quadrant).

There were no clear cases of galaxies that were actually stars, based on their proper motion, or stars that should be galaxies.

TABLE 14. Information about Coordinate Transformations for UMa I

Fi- eld (1)	N _s (2)	N _m (3)	σ_a (pixel) (4)	N _f (5)	χ^2 (6)	N _{dof} (7)	P(χ^2) (8)	$\sigma_{\langle \mu \rangle, x}$ (10 ⁻³ pixel yr ⁻¹) (9)	$\sigma_{\langle \mu \rangle, y}$ (10)
1s	24	20	0.0060	12	31.77	28	0.284	1.14	1.16
1t	27	19	0.0060	12	31.92	26	0.196	1.06	1.11
2s	71	63	0.0025	12	76.54	114	0.997	0.74	0.82
2t	31	25	0.0050	12	38.11	38	0.465	1.48	1.44

The data in Table 14 show that there are some issues with the transformations between epochs, particularly for Fields 1s and 1t. For those fields even relatively large additional uncertainties did not make the χ^2 less than or equal to the number of degrees of freedom. Still larger additive uncertainties changed more non-member stars into members and the χ^2 remains larger than the number of degrees of freedom. It is possible that the small number of stars is making it difficult to distinguish between members and non-members. However, I lowered the S/N limit on stars in the gpf program for Field 1t and got 5 more stars. These were all classified as members, though their motions seem very noisy (χ^2 is still above N_{dof}). The proper motion derived from the field change by much less than 1σ , so this test does not indicate any obvious problem with the measured proper motion.

Averaging the galaxy motions in the different fields produced the results in Table 15. The individual measurements within Field 1 and Field 2 do not agree very well.

TABLE 15. Information on Raw UMa I Proper Motions

Fi- eld (1)	N _g (2)	μ_x (10 ⁻³ pixel yr ⁻¹) (3)	μ_y (4)	M ₄ (5)	S/N x/y (6)	M ₃ (7)	S/N x/y (8)	M ₂ (9)	S/N x/y (10)	M ₁ (11)
1q	1	-23.38 ± 3.15	$+3.58 \pm 3.68$							
1s	83	-16.05 ± 1.68	$+14.33 \pm 2.29$	1.40/2.09	15.2	1.47/2.08	20.4	1.33/1.99	29.3	1.41/1.76
1t	91	-12.77 ± 1.66	$+10.11 \pm 1.52$	1.78/2.22	14.7	1.26/1.57	20.4	1.99/1.29	30.5	1.34/1.16
2q	1	$+19.88 \pm 2.50$	-11.25 ± 2.24							
2s	138	$+20.34 \pm 1.88$	-5.15 ± 1.63	2.00/2.65	13.0	1.71/2.03	16.2	2.17/2.08	25.5	1.29/0.98
2t	102	$+24.60 \pm 1.93$	$+0.43 \pm 1.88$	1.61/1.41	13.2	1.99/1.56	16.6	1.29/1.87	25.8	1.16/1.13

Converting the raw motions into proper motions yields the results in Table 16. The uncertainties in the zero-point of the stellar reference frame are not entirely negligible compared to the uncertainty from the mean galaxy motion. Thus, the two uncertainties were added in quadrature for both fields before converting to (μ_α, μ_δ) .

TABLE 16. Measured Proper Motions
for UMa I

Field	Δt (yrs)	μ_α (mas century $^{-1}$)	μ_δ (mas century $^{-1}$)
(1)	(2)	(3)	(4)
1q	2.990	-81.0 ± 24.0	-47.9 ± 26.6
1s	"	-37.9 ± 14.8	-76.7 ± 17.5
1t	"	-32.0 ± 13.7	-56.3 ± 13.3
2q	1.983	-36.8 ± 17.7	-83.1 ± 17.3
2s	"	-52.7 ± 13.7	-64.7 ± 13.3
2t	"	-79.5 ± 17.6	-57.0 ± 18.0
mean		-48.8 ± 6.5	-65.0 ± 6.7

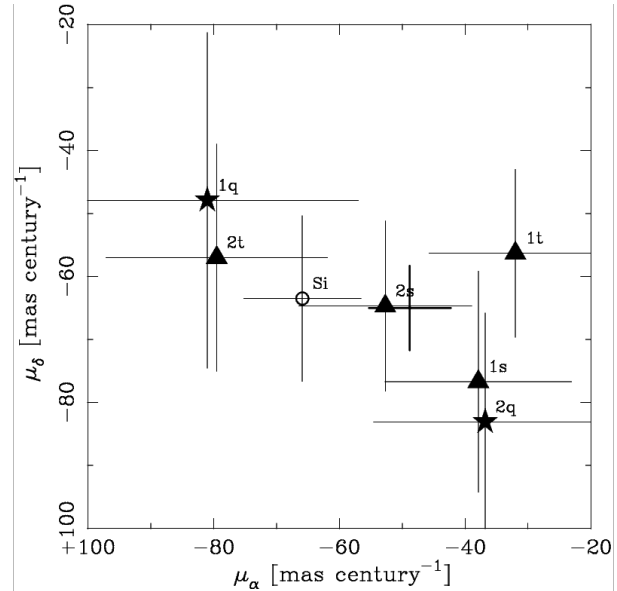


Figure 20. Individual proper motion measurements for UMa I. Also shown as an open circle is the measurement by Simon (2018).

The scatter of the individual measurements around their mean is larger than expected from the uncertainties and much more so than for previous galaxies in this summary. Multiplying the uncertainties by 1.76 produced a χ^2 per degree of freedom of one for μ_α and μ_δ combined. The uncertainties listed in Table 16 and plotted in Figure 20 have been multiplied by that factor.

Also plotted in Figure 20 are the measurements using the Gaia DR2 data from Simon (2018) of $(\mu_\alpha, \mu_\delta) = (-65.9 \pm 9.3, -63.5 \pm 13.1)$ mas century $^{-1}$. The agreement of this value with our mean is OK, with the two μ_α values differing by 17.1 ± 11.3 mas century $^{-1}$ – which is 1.5σ . The difference between the two measurements is similar in size and direction to that seen for Boo I, but is less significant.

The origin of the larger-than-usual scatter among our measurements from different fields may just be systematic errors induced by the small numbers of stars in the fields. However, given the strong elongation of UMa I and the separation of our two fields along the major axis, it is worth considering whether internal motions could be contributing. The mean proper motion of our three measurements for Field 1 is $(\mu_\alpha, \mu_\delta) = (-41.7 \pm 9.8, -61.6 \pm 10.3)$ mas century $^{-1}$ and for Field 2 is $(\mu_\alpha, \mu_\delta) = (-55.8 \pm 9.4, -67.8 \pm 11.4)$ mas century $^{-1}$. The difference is not statistically significant, so these numbers do not provide any evidence for internal motions. The difference in the two proper motions corresponds to 71 km s $^{-1}$ at the distance of UMa I. That seems too large to be ascribable to internal motions. It would be interesting to look at the Gaia DR2 data for evidence of a velocity gradient along the long axis, but Simon (2018) has a sample of only 8 stars, so it is unlikely that anything will be detectable.